Hindawi
Evidence-Based Complementary and Alternative Medicine
Volume 2022, Article ID 5643345, 14 pages
https://doi.org/10.1155/2022/5643345

Research Article

Prediction of the Active Components and Mechanism of *Forsythia suspensa* Leaf against Respiratory Syncytial Virus Based on Network Pharmacology

Xiaoxue Wang,[1] Ping Wang,[2,3] Haitao Du,[1] Na Li,[1] Tianyuan Jing,[1] Ru Zhang,[1] Wanying Qi,[1] Yanan Hu,[1] Tianyu Liu,[4] Lanxin Zhang,[5] Nan Xu,[2] Yi Wang,[2] Huimin Zhang,[2] and Xiaoyan Ding[2]

[1]*College of Pharmacy, Shandong University of Traditional Chinese Medicine, Jinan, Shandong, China*
[2]*Shandong Academy of Chinese Medicine, Jinan, Shandong, China*
[3]*State Key Laboratory of Precision Testing Technology and Instruments, Tianjin University, Tianjin, China*
[4]*Shanghai International Studies University, Shanghai, China*
[5]*Macau University of Science and Technology, Macau, China*

Correspondence should be addressed to Ping Wang; wangpingjinan@163.com, Yi Wang; 871916401@qq.com, and Xiaoyan Ding; kate-66@163.com

Xiaoxue Wang, Ping Wang, and Haitao Du contributed equally to this work.

Received 8 April 2022; Revised 20 May 2022; Accepted 31 May 2022; Published 20 July 2022

Academic Editor: Chan-Yen Kuo

Objective. *Forsythia suspensa* leaf (FSL) has been used as a health tea in China for centuries. Previous experiments have proved that FSL extract has a good effect on the antirespiratory syncytial virus (RSV) *in vitro*, but its exact mechanism is not clear. Therefore, this study aims to determine the active components and targets of FSL and further explore its anti-RSV mechanism. *Methods*. UPLC-Q-Exactive-MS was used to analyze the main chemical components of FSL. The compound disease target network, PPI, GO, and KEGG were used to obtain key targets and potential ways. Then, the molecular docking was verified by Schrödinger Maestro software. Next, the cell model of RSV infection was established, and the inhibitory effect of each drug on RSV was detected. Finally, western blotting was used to detect the effect of the active components of FSL on the expression of PI3K/AKT signaling pathway-related protein. *Results*. UPLC-Q-Exactive-MS analysis showed that there were 67 main chemical constituents in FSL, while network pharmacological analysis showed that there were 169 anti-RSV targets of the active components in FSL, involving 177 signal pathways, among which PI3K/AKT signal pathway played an important role in the anti-RSV process of FSL. The results of molecular docking showed that cryptochlorogenic acid, phillyrin, phillygenin, rutin, and rosmarinic acid had higher binding activities to TP53, STAT3, MAPK1, AKT1, and MAPK3, respectively. *In vitro* experiments showed that phillyrin and rosmarinic acid could effectively improve the survival rate of RSV-infected cells, increase the expression level of PI3K, and decrease the expression level of AKT. *Conclusion*. The active ingredients of FSL, phillyrin, and rosmarinic acid can play an anti-RSV role by inhibiting PI3K/AKT signaling pathway. This study provides reliable theoretical and experimental support for the anti-RSV treatment of FSL.

1. Introduction

The vulnerable part of the human body is the respiratory tract, most of which are caused by viruses, so viral respiratory diseases have become the most common infectious diseases in human beings. The outbreak of COVID-19 at the end of 2019 clearly shows the high risk of viral infection. Respiratory syncytial virus (RSV), one of the most common respiratory viruses, is named as it can cause fusion lesions in respiratory tissue culture cells [1]. RSV is a negative single-stranded RNA virus of the family Paramyxoviridae, and is also the main pathogen of early acute respiratory infection in children [2]. Epidemiological investigation shows that RSV infection has certain seasonality. Infants, children, and

elderly people with low immunity are vulnerable to infection. Without specific immunity after infection, there is a risk of reinfection [2–4]. More than 30 million children in the world are infected with RSV each year, but there is no specific therapeutic drug or preventive vaccine at present. Ribavirin, a broad-spectrum antiviral drug, has a certain inhibitory effect on RSV, however, with serious adverse reactions, such as myelosuppression and carcinogenicity; it is limited in clinical use [5].

Traditional Chinese medicine has long played a unique role in the treatment of viral infectious diseases because of its multicomponent and multitarget advantages. Traditional heat-clearing drugs, including Scutellaria baicalensis, Coptis chinensis and Forsythia suspensa have been proved to have a significant anti-RSV effect [6–8]. In recent years, studies have shown that the chemical constituents in the leaves and fruits of Forsythia suspensa are very similar, and the content of phillyrin in the leaves of Forsythia is even 40 times higher than that in the fruits of *Forsythia suspensa* [9], which reveals that the leaves of Forsythia suspensa have a potential anti-RSV effect. *Forsythia suspensa* leaf (FSL) comes from the compendium of materia medica, has a bitter taste, cold nature, and the effect of heat-clearing and detoxification. In addition, in the Yuqiao Medical Order, it is written that FSL is bitter, slightly pungent, cold in nature, can be used to relieve fire, clear heat, and benefit the heart and lung meridians. At present, more than 200 chemical constituents have been isolated and extracted from FSL. The main active components are phillyrin, phillygenin, rutin, chlorogenic acid, and caffeic acid, they have pharmacological effects, for instance, antibacterial, antiviral, liver protection, heart protection, antioxidation and so on [10–13]. *Forsythia suspensa* is usually used in medicine with fruit, which has a wide range of functions and a long history in medicine. Nevertheless, a large number of FSLs are discarded. The development and utilization of FSL are limited to the application of Forsythia tea in a small number of areas [14], which is a great waste of resources. Therefore, exploring the anti-RSV mechanism of the active components in FSL is not only conducive to the research and development of new anti-RSV drugs, but also provides a theoretical basis for the development and utilization of FSL.

Network pharmacology is a new research tool that comprehensively analyzes drugs, disease-related genes, and proteins in a bioinformatics database. It has been widely used in the research of traditional Chinese medicine, and it is of great significance to reveal the action mechanism of active ingredients of traditional Chinese medicine [15]. In addition, molecular docking is a means of further analysis based on the prediction of network pharmacology, which can study the interaction between ligand and receptor by simulating the interaction between molecules and the binding mode of both, so as to evaluate the binding potential of protein ligand [16]. Nowadays, using network pharmacology to clarify the potential mechanism of complex components through big data analysis and molecular docking simulation has become a common method to study the pharmacological mechanism of traditional Chinese medicine. Previous experiments conducted by our research group showed that the extract of FSL had a positive anti-RSV effect *in vitro*. In this study, the possible molecular mechanism between chemical components and disease targets of FSL was explored by network pharmacology, verified by molecular docking and *in vitro* experiments, and its action mechanism was explored by Western blot, providing a scientific basis for the further study of the material basis and molecular mechanism of anti-RSV in FSL.

2. Material and Methods

2.1. Chemical Composition Analysis of FSL. FSL was harvested from Shandong University of Traditional Chinese Medicine in April and identified by researcher Lin Huibin of Institute of Traditional Chinese Medicine Resources, Shandong Academy of Chinese Medicine as the leaves of *Forsythia suspensa* (Thunb.) Vahl, family Lignanaceae. The leaves were dried at room temperature, crushed, and preserved. Weighing 20 g FSL and adding water (1 : 10) to soak them for 2 h, then heating and refluxing twice, 1 h for each. The extract was combined, filtered, and concentrated to 1 g/mL as the original medicinal material, and stored in the refrigerator at −20°C. 1 mL solution was added to methanol at a constant volume of 100 mL. The supernatant was obtained by ultrasonic for 30 min, 6000 rpm centrifugation for 10 min, and then passed through a 0.22 μm filter membrane. The chemical constituents of FSL were analyzed by UPLC-Q-Exactive-MS. In comparison to the literature, the compounds obtained were qualitatively analyzed, and the main chemical constituents of FSL were screened.

2.2. Target Acquisition of FSL. Firstly, the information of compounds and molecules was obtained by the PubChem database [17, 18] (https://pubchem.ncbi.nlm.nih.gov/), and the smile information of compounds was uploaded to the Swiss TargetPrediction database [19–21] (http://www.swisstargetprediction.ch/) to predict the target of compounds. UniProt database [22, 23] (https://www.uniprot.org/) was used to normalize the gene information, and the target with Probability > 0 was selected for the study. Comparing the target genes of the main active components of FSL with the targets related to Respiratory Syncytial Virus found in databases such as GeneCards [24, 25] (http://www.genecards.org/) and OMIM [26, 27] (https://omim.org/), the obtained repeated targets are the potential targets of the main active components of FSL against the respiratory syncytial virus. Using Cytoscape software (version 3.7.1) [28, 29], the network diagram of active components-targets of FSL was constructed.

2.3. Construction of Compound Targeting Pathway Network of FSL. The potential targets of FSL against RSV were introduced into the string platform [30, 31] (https://string-db.org/) to construct a functional PPI analysis (confidence is 0.7). Then, KEGG pathway analysis and gene ontology biological process analysis were carried out by DAVID Bioinformatics Resources (https://david.ncifcrf.gov/) [32, 33], and the correlation analysis results were obtained ($P < 0.05$).

The KEGG pathway analysis results were visualized by using OmicShare tools [34,35].

2.4. Molecular Docking. Firstly, 3D structures of 67 chemical components were obtained from the PubChem database. Then, using the PDB database (https://www.rcsb.org/) and Uniprot database (https://www.uniprot.org/) [36], the target protein crystal structure TP53 with high resolution (Å) and complete structure TP53 (PDB ID : 1YC5, The resolution is 1.4 Å), STAT3(PDB ID : 6NJS, resolution 2.70 Å), MAPK1(PDB ID : 2Y9Q, resolution 1.55 Å), AKT1(PDB ID : 1UNQ, resolution 0.98 Å) and MAPK3(PDB ID : 4QTB, resolution 1.40 Å). Molecular docking was performed by Schrödinger Maestro software (version free) [37]. Use LigPrep and Protein Preparation Wizard plug-ins to pretreat ligand molecules and target proteins, hydrogenate proteins, remove water molecules, and charge them; The receptor grid generation plug-in is used to generate the target protein grid file, and all amino acid residues within the radius of 10 are used as active cavities; Finally, the ligand docking plug-in is used to dock the ligand molecule with the target protein, and the docking diagram and docking score are output to evaluate the docking of the receptor and the ligand.

2.5. Cells and Viruses. Respiratory syncytial viruses (RSV, Institute of Basic Medical College, Shandong Academy of Medical Sciences, Shandong, China) were amplified from human laryngeal epidermoid cancer cells (HEp-2; Institute of Basic Medical College, Shandong Academy of Medical Sciences, Shandong, China). The cells were cultured in a humidified incubator (5% CO_2, 37°C) with a DMEM medium containing 10% fetal bovine serum and antibiotics. 50% histiocytic infection dose ($TCID_{50}$) of the virus was determined. The virus was stored in a refrigerator at −80°C.

2.6. Anti-RSV Efficacy of the Active Ingredients of Forsythia Suspense Leaf. Taking a 96-well plate covered with monolayer HEp-2 cells, five standard drugs (five compounds with the best molecular docking fraction in 2.5) with 2 times dilution, water extract of FSL and ribavirin were added to the plate. Normal cells were set as control and cultured at 37°C in a 5%CO_2 incubator for 24 h. MTT [38] (Thiazolyl Blue Tetrazolium Bromide, 3-(4,5-Dimethylthiazol-2-yl)-2,5-diphenyltetrazolium bromide) was used to measure $OD_{490\,nm}$ and determine the maximum nontoxic concentration of each drug.

The 96-well plates full of monolayer HEp-2 cells were divided into the normal group, model group, ribavirin group, and drug group. Except for the normal group, the other groups were added with 50 μL of RSV virus of 100$TCID_{50}$. In the drug group, 50 μL of each series of drugs diluted by 2 times were added, with a total of 8 concentrations, and 6 multiple wells were set up. In the virus group and the normal group, 2% cell maintenance solution, 50 μL/well, and 100 μL/well were added, respectively. They were cultured in an incubator and observed daily, and the $OD_{490\,nm}$ value was measured by MTT at 24 and 48 hours after infection. The cell survival rate of each drug group was calculated.

2.7. Effect of Drugs on PI3K/AKT Signaling Pathway in HEp-2 Cells by Western Blot. The HEp-2 cells of each group were collected, and the total protein was extracted with RIPA lysate (Solarbio, Beijing, China). The standard curve was drawn, and the protein content was determined according to the instructions of the BCA kit (Solarbio, Beijing, China). Based on the differences in the relative molecular weight of proteins, 7.5%–12.5% SDS-PAGE gel electrophoresis was performed. After electrophoresis, the protein was transferred to the PVDF membrane, sealed in 5% defatted milk powder at room temperature for 3 h, and the target molecule-specific primary antibodies were incubated overnight at 4°C. The first antibodies included PI3K (1 : 1000), *p*-PI3K (1 : 1000), AKT (1 : 2000), *p*-AKT (1 : 1500) (Abcam, UK), *β*-Actin (1 : 1000) (Cell Signaling Technology, USA). After 1 × TBST washing, antirabbit IgG labeled with horseradish peroxidase (Zhongshanjinqiao, Beijing, China) was incubated at room temperature for 1 h. The protein bands were developed with ECL photoluminescence solution, and the experimental results were analyzed by Image J software (version 1.8.0) [39].

2.8. Statistical Analysis. The experimental data were analyzed by IBM SPSS Statistics software (version 28.0) [40]. Each independent experiment was repeated at least three times to obtain the average value, and the data were expressed as the mean ± standard deviation. One-way ANOVA and LSD multiple comparison analysis were used for comparison among multiple groups, and $P < 0.05$ indicated that the difference was statistically significant.

3. Result

3.1. Determination of Chemical Constituents of FSL. UPLC-Q-Exactive-MS was used to identify and analyze the main chemical components of FSL water extract. A total of 67 compounds were obtained by comparing the relative molecular weight information of compounds provided by mass spectrometry with known databases and references, it mainly includes caffeic acid, phillyrin, (+) - rosin-beta-d-glucopyranoside, calceolarioside B, forsythin glycoside B, and rutin (Table 1).

3.2. Active Ingredient Targets Prediction. In this study, a total of 2952 potential targets for FSL and 849 RSV disease targets were obtained. After comparison and analysis with potential targets for FSL, 169 potential targets for anti-RSV of FSL were obtained, mainly including matrix metalloproteinase 2 (MMP2), mitogen-activated protein kinase activated protein kinase 2 (MAPKAPK2), and cyclin-dependent kinase 1 (CDK1). The intersection targets and their component relationships are imported into Cytoscape 3.7.1 for visualization, forming a network of "active components

Table 1: Main hemical composition of FSL.

NO.	Compound	Molecular formula	Ion mode	Mzmed	RT/min	Peak area
1	(+)-Pinoresinol	$C_{20}H_{22}O_6$	$[M-H]^-$	357.13	6.56	791229617.70
2	(+)-Pinoresinol-4-O-beta-D-glucopyraside	$C_{26}H_{32}O_{11}1$	$[M-H]^-$	519.19	6.56	4166509751.00
3	Salidroside	$C_{14}H_{20}O_7$	$[M-H]^-$	299.11	2.98	416030123.60
4	Quercetin	$C_{15}H_{10}O_7$	$[M+H]^+$	303.05	6.60	883627.57
5	Hyperoside	$C_{21}H_{20}O_{12}2$	$[M-H]^-$	463.08	6.08	7594792.25
6	Caffeic acid	$C_9H_8O_4$	$[M-H]^-$	179.03	4.01	10694238742.00
7	Phillyrin	$C_{27}H_{34}O_{11}1$	$[M-H]^-$	579.20	7.73	7458440880.00
8	Chlorogenic acid	$C_{16}H_{18}O_9$	$[M-H]^-$	353.08	3.57	110358675.20
9	Kaempferol	$C_{15}H_{10}O_6$	$[M-H]^-$	285.03	8.89	355385.01
10	3-Hydroxybenzaldehyde	$C_7H_6O_2$	$[M-H]^-$	121.02	4.21	188945020.50
11	Ferulic acid	$C_{10}H_{10}O_4$	$[M-H]^-$	193.04	4.49	4914965.43
12	P-Hydroxyphenyl acrylic acid	$C_9H_8O_3$	$[M-H]^-$	163.03	4.65	10697330.91
13	Secoisolariciresinol	$C_{20}H_{26}O_6$	$[M-H]^-$	361.16	7.09	9828539.83
14	Calceolarioside B	$C_{23}H_{26}O_{11}1$	$[M+H]^+$	479.16	5.89	675251118.64
15	Vanillic acid	$C_8H_8O_4$	$[M-H]^-$	167.03	3.94	48787513.71
16	4-Dicaffeoylquinic acid	$C_{16}H_{18}O_9$	$[M-H]^-$	353.08	3.88	80843996.30
17	Quinic acid	$C_7H_{12}O_6$	$[M-H]^-$	191.05	4.57	57466022.97
18	3,4-Dihydroxybenzaldehyde	$C_7H_6O_3$	$[M-H]^-$	137.02	4.00	60332307.59
19	Phillyrin B	$C_{34}H_{44}O_{19}9$	$[M-H]^-$	755.23	6.00	820467980.90
20	4-Hydroxycinnamic acid	$C_9H_8O_3$	$[M-H]^-$	163.03	5.27	250776002.80
21	Rhamnocitrin	$C_{20}H_{22}O_6$	$[M-H]^-$	357.13	27.22	22984449.73
22	P-hydroxybenzoxal	$C_7H_6O_2$	$[M-H]^+$	123.04	0.87	24287717.24
23	Benzoic acid	$C_7H_6O_2$	$[M+H]^+$	123.04	3.64	40801996.94
24	Isophorone	$C_9H_{14}O$	$[M-H]^+$	139.11	2.79	116897843.36
25	Nivolumab	$C_8H_8O_3$	$[M+H]^+$	153.06	5.21	62982567.92
26	Camphor	$C_{10}H_{16}O$	$[M+H]^+$	153.13	5.84	106102205.21
27	Tryptamine	$C_{10}H_{12}N_2$	$[M+H]^+$	161.11	26.80	7964958.56
28	2-Coumarin	$C_9H_8O_3$	$[M+H]^+$	165.06	3.83	43963794.17
29	P-Hydroxycinnamic acid	$C_9H_8O_3$	$[M+H]^+$	165.06	4.58	9310132.79
30	Paeonol	$C_9H_{10}O_3$	$[M+H]^+$	167.07	3.22	30106741.86
31	Homogentisic acid	$C_8H_8O_4$	$[M+H]^+$	169.05	1.24	89280908.15
32	Geranic acid	$C_{10}H_{16}O_2$	$[M+H]^+$	169.12	1.02	56272751.98
33	6,7-Dihydroxy-4-methylcoumarin	$C_{10}H_8O_4$	$[M+H]^+$	193.05	7.40	11318256.46
34	Scopolactone	$C_{10}H_8O_4$	$[M+H]^+$	193.05	0.45	6146412.70
35	Yokogawa ligustilide A	$C_{12}H_{16}O_2$	$[M+H]^+$	193.12	8.71	9992106.14
36	Dihydrokaempferol (colombian aglycone)	$C_{14}H_{14}O_4$	$[M+H]^+$	285.05	1.74	1054100.46
37	Propethrin	$C_{19}H_{26}O_3$	$[M+H]^+$	303.20	7.44	37631362.46
38	Sanguinarine	$C_{15}H_{10}O_7$	$[M+H]^+$	303.05	8.10	44076.10
39	Boswellic acid	$C_{20}H_{30}O_2$	$[M+H]^+$	303.23	12.14	3471892.58
40	(-)-Epigallocatechin	$C_{15}H_{14}O_7$	$[M+H]^+$	307.08	6.12	282532593.99
41	Gallocatechins	$C_{15}H_{14}O_7$	$[M+H]^+$	307.08	4.69	7539336.66
42	Caffeinol	$C_{20}H_{28}O_3$	$[M+H]^+$	317.21	10.82	33616062.68
43	Isorhamnetin	$C_{16}H_{12}O_7$	$[M+H]^+$	317.07	6.46	1930112.37
44	Ginkgoneolic acid	$C_{20}H_{32}O_3$	$[M+H]^+$	321.24	11.45	8274443.51
45	Isoform aconitin	$C_{20}H_{27}NO3$	$[M+H]^+$	330.21	6.89	17743758.07
46	Columbin	$C_{20}H_{22}O_6$	$[M+H]^+$	359.15	6.13	15304281.36
47	Genistein B	$C_{19}H_{18}O_7$	$[M+H]^+$	359.11	1.14	98701853.52
48	Rosmarinic acid	$C_{18}H_{16}O_8$	$[M+H]^+$	361.09	4.57	400615.12
49	Curcumin	$C_{21}H_{20}O_6$	$[M+H]^+$	369.13	9.96	5345129.23
50	Aucubin	$C_{15}H_{22}O_9$	$[M+H]^+$	369.12	2.21	3112265.84
51	Forsytheins	$C_{21}H_{24}O_6$	$[M+H]^+$	373.17	7.78	81425864.68
52	Paraphyllin	$C_{22}H_{33}NO4$	$[M+H]^+$	376.25	4.94	21317926.78
53	Loganic acid	$C_{16}H_{24}O_{10}0$	$[M+H]^+$	377.15	4.69	61961252.11
54	Eleutheroside	$C_{16}H_{22}O_9$	$[M+H]^+$	381.12	2.97	39828726.65
55	Pseudolaric acid C	$C_{21}H_{26}O_7$	$[M+H]^+$	391.18	8.97	33835218.13
56	Afzelin	$C_{21}H_{20}O_{10}0$	$[M+H]^+$	433.11	6.37	1241906.35
57	Astragalin	$C_{21}H_{20}O_{11}1$	$[M+H]^+$	449.11	6.19	5731468.55
58	Isosakuranin	$C_{22}H_{24}O_{10}0$	$[M+H]^+$	449.15	3.63	58302445.74
59	Asperuloside acid	$C_{18}H_{24}O_{12}2$	$[M+H]^+$	455.12	4.25	1549292.02
60	Berberine	$C_{26}H_{30}O_7$	$[M+H]^+$	455.20	7.44	653736.80

Table 1: Continued.

NO.	Compound	Molecular formula	Ion mode	Mzmed	RT/min	Peak area
61	Forsythoside E	$C_{20}H_{30}O_{12}2$	$[M+H]^+$	463.18	3.20	119659925.90
62	Methylnissolin-3-O-glucoside	$C_{23}H_{26}O_{10}0$	$[M+H]^+$	463.16	6.75	6053442.72
63	Isoquercitrin	$C_{21}H_{20}O_{12}2$	$[M+H]^+$	465.10	6.10	35289037.57
64	Daphylloside	$C_{19}H_{26}O_{12}2$	$[M+H]^+$	469.13	5.22	125152971.49
65	Calceolarioside A	$C_{23}H_{26}O_{11}1$	$[M+H]^+$	501.14	3.20	29042008.47
66	Rutin	$C_{27}H_{30}O_{16}6$	$[M+H]^+$	611.16	5.92	799317923.21
67	Isorhamnetin-3-o-neohesperidin	$C_{28}H_{32}O_{16}6$	$[M+H]^+$	625.18	6.45	3038686.75

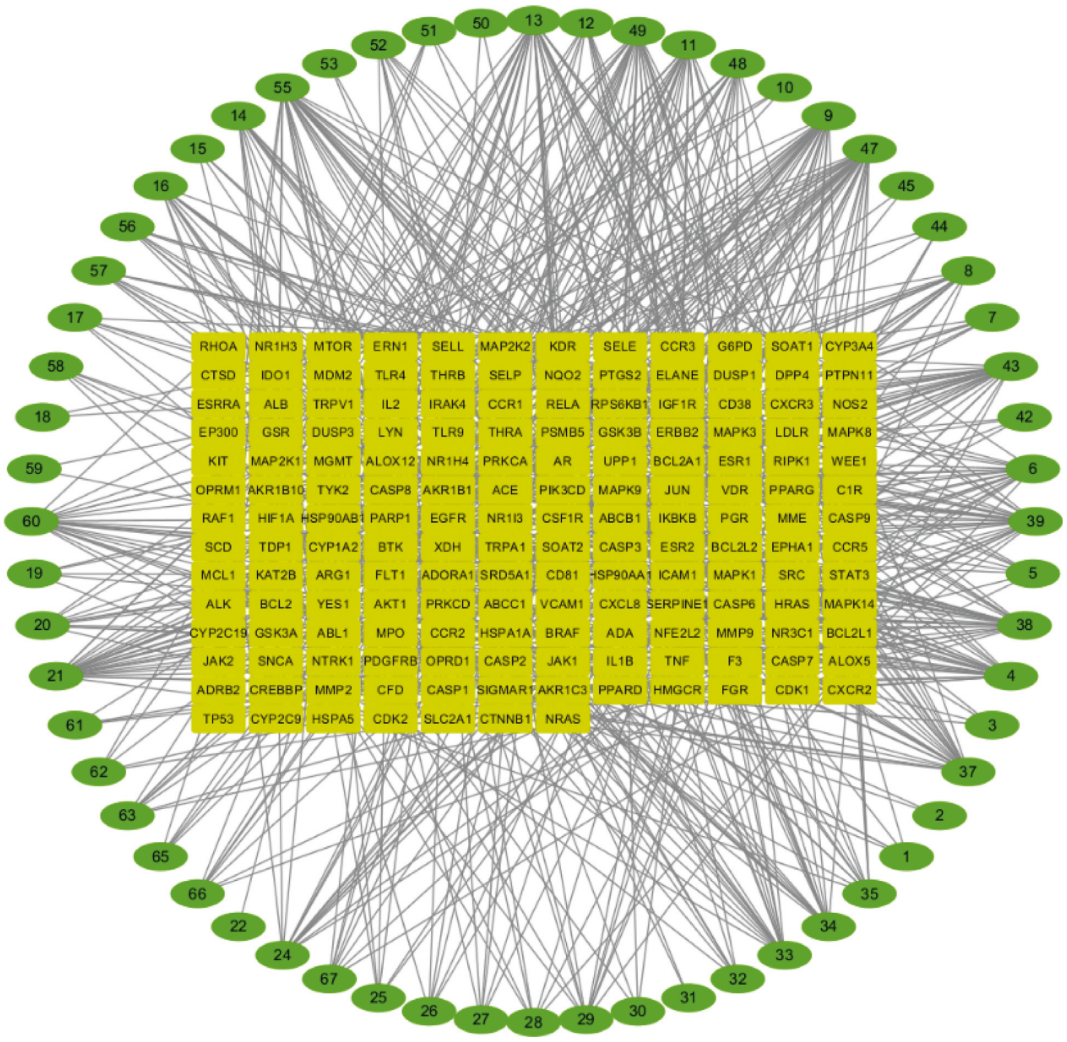

Figure 1: Active ingredient of FSL-RSV pneumonia target network.

of FSL-RSV pneumonia targets." The gene network has 223 nodes and 683 edges in total (Figure 1).

3.3. Structure Protein-Protein Interaction (PPI) Network. Nodes were evaluated and colored by node degree values, the anti-RSV protein-protein interaction network diagram of FSL was obtained (Figure 2(a)). The network diagram contains 155 targets and 1330 edges. The larger the degree value is, the larger the node is. The protein with a large degree value (degree value > 50) is TP53, STAT3, MAPK1, AKT1, MAPK3, MAPK8, SRC, and TNF. Through the PPI network diagram, we can intuitively discover the complex interactive relationship between compounds and targets, and further, characterize the synergistic regulation of anti-RSV by FSL by multicomponent and multitarget features.

The DAVID database was used to analyze the anti-RSV targets of the main components of FSL by GO and KEGG. The results of GO analysis show that FSL mainly takes effects by regulating the following biological processes: under the condition of $P < 0.05$, 475 BP (Bioprogress, cell biological processes, such as adhesion, migration, and apoptosis,

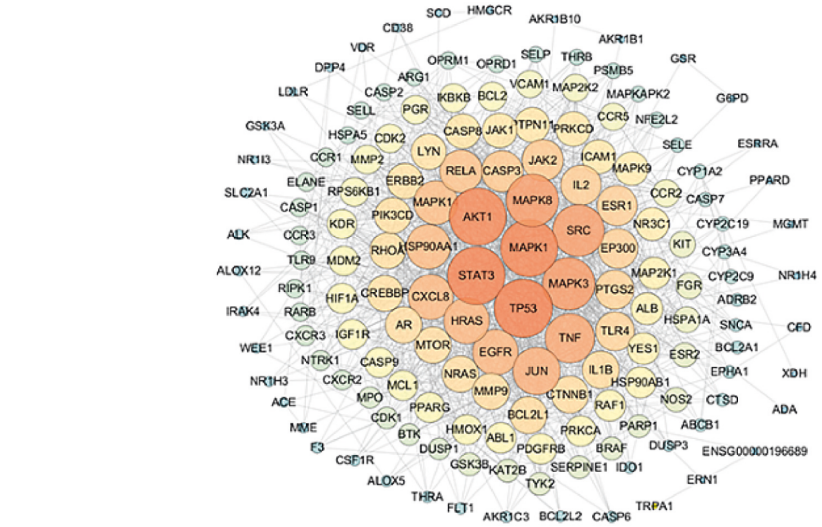

(a)

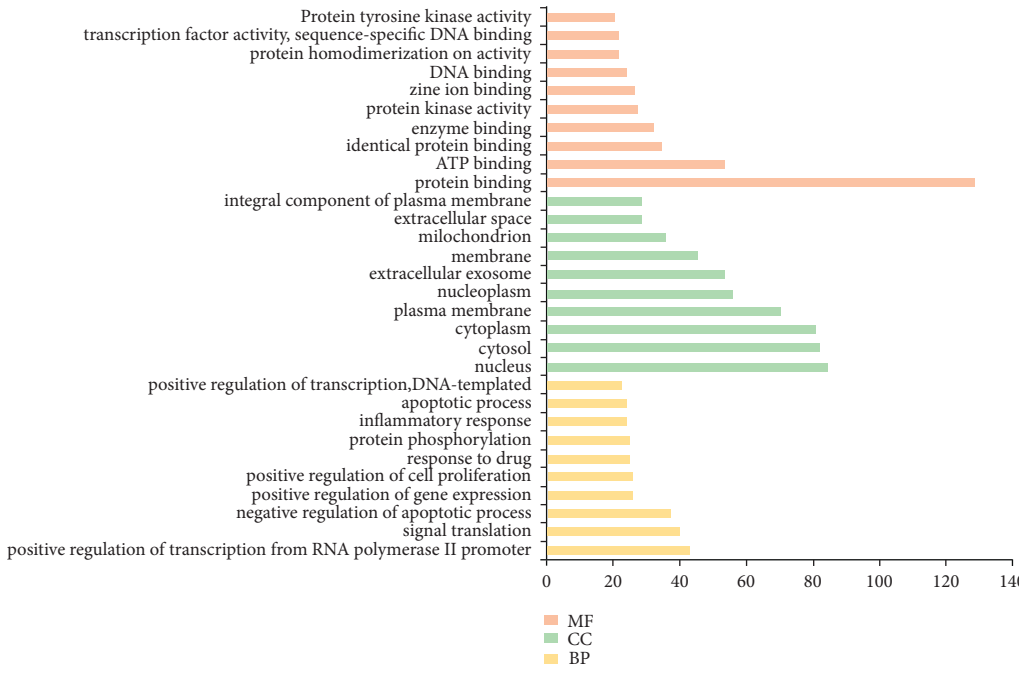

(b)

Figure 2: Continued.

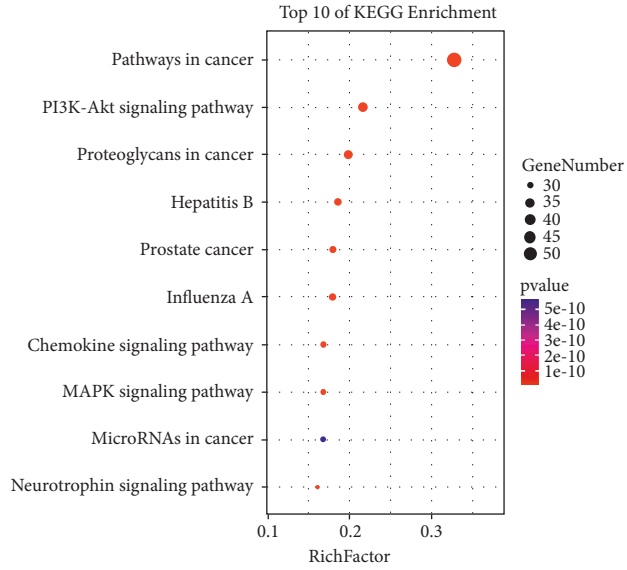

(c)

Figure 2: (a) PPI network of FSL anti-RSV; (b) GO enrichment analysis of anti-RSV target biological processes of FSL; (c) bubble diagram of KEGG enrichment pathway, the main target of FSL.

cycle.), 59 CC (Cell Components, cell composition, such as cell membrane and cytoplasm.), 132 MF (Molecular Function) (Figure 2(b), ranked according to Count, the top 10), and 30 pathways were selected. There are 10 signaling pathways in KEGG analysis, among which Pathways in cancer, PI3K/AKT signaling pathway, Proteoglycans in cancer, Hepatitis B, and other four pathways have large nodes, which may be an important pathway for Forsythia suspense leaf to play an anti-RSV role. 10 pathways are visualized by sorting according to the number of target hits (Figure 2(c)).

3.4. Molecular Docking. Schrödinger molecular docking module provides SP (standard precision) and XP (extra precision) to ensure the speed and accuracy of docking results. Moreover, the contribution of hydrogen bond, lipophilicity, and metal ligand, as well as the rotation of unsuitable bonds and atoms with steric repulsion will be fully considered in the docking score to ensure the reliability of the results. The 67 compounds selected under 2.1 were molecularly docked with five potential target proteins with network node (degree) > 56. The larger the absolute value of the docking score, the greater the affinity of docking between ligand and receptor. When the absolute value of docking score is greater than 5.0, it indicates that there is a strong interaction between the compound and the target protein, and the binding configuration of the compound and the target has a strong activity. The docking score results are shown in Table 2, which lists five compounds with high binding activity with five target proteins. The results showed that cryptochlorogenic acid, phillyrin, phillygenin, rutin, and rosmarinic acid had a high binding activity with TP53, STAT3, MAPK1, AKT1, and MAPK3, respectively. The docking mode diagram is shown in Figure 3. Therefore, cryptochlorogenic acid, phillyrin, phillygenin, rutin, and rosmarinic acid were selected for pharmacodynamic verification.

Table 2: FSL compounds-potential target proteins docking score.

Target	Compound	Docking Score
TP53 (PDB ID : 1YC5)	Cryptochlorogenic acid	−8.146
	Phenyl sthanol glucoside B	−7.619
	Rosmarinic acid	−7.617
	Phenethyl acetate	−7.608
	Aucubin	−7.533
STAT3 (PDB ID : 6NJS)	Phillyrin	−5.269
	P-Hydroxyphenyl acrylic	−4.966
	4-Hydroxycinnamic acid	−4.966
	Paeonol	−4.966
	Vanillic acid	−4.907
MAPK1(PDB ID : 2Y9Q)	Phillygenin	−8.627
	Phenethyl acetate	−8.602
	Cryptochlorogenic acid	−8.362
	Quercetin	−8.353
	Loganine acid	−8.206
AKT1(PDB ID: 1UNQ)	Rutin	−6.057
	Vanillic acid	−5.956
	Dextroquinic acid	−5.854
	Dihydrobehenyl alcohol	−5.756
	Methyl paraben	−5.611
MAPK3(PDB ID: 4QTB)	*Rosmarinic acid*	−7.383
	Phillyrin	−7.129
	Cryptochlorogenic acid	−6.783
	Phenethyl acetate	−6.758
	Salidroside	−6.744

TP53, tumor protein p53; STAT3, signal transducer and activator of transcription 3; MAPK1, mitogen-activated

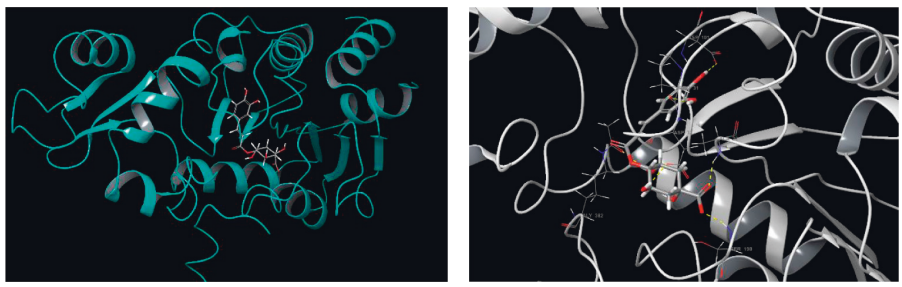

TP53-Cryptochlorogenic acid

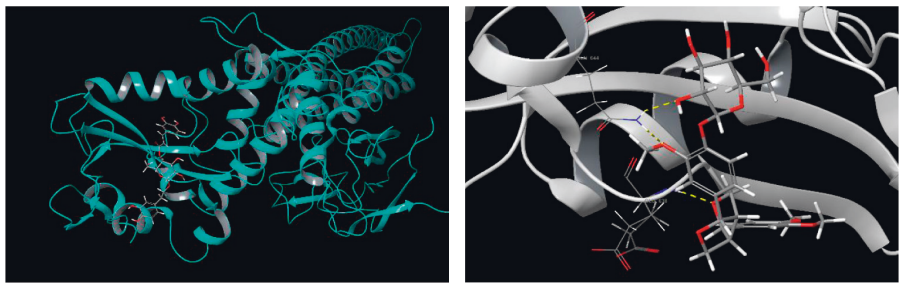

STAT3-Phillyrin

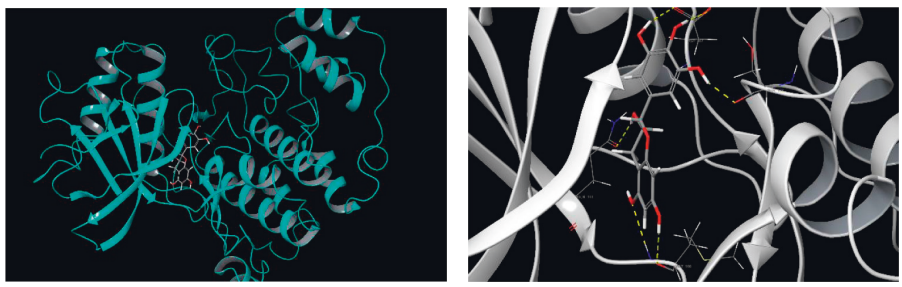

MAPK1-Phillygenin

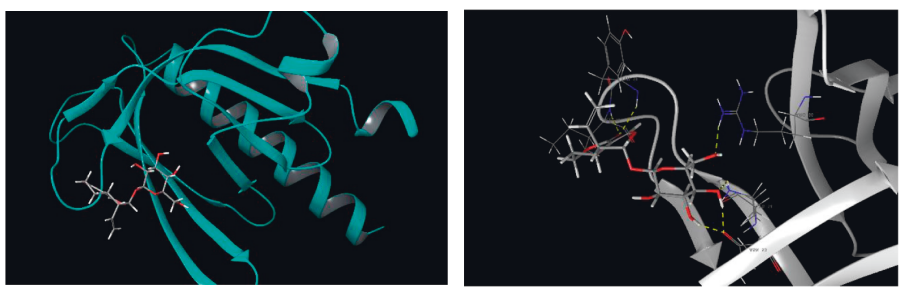

AKT1-Rutin

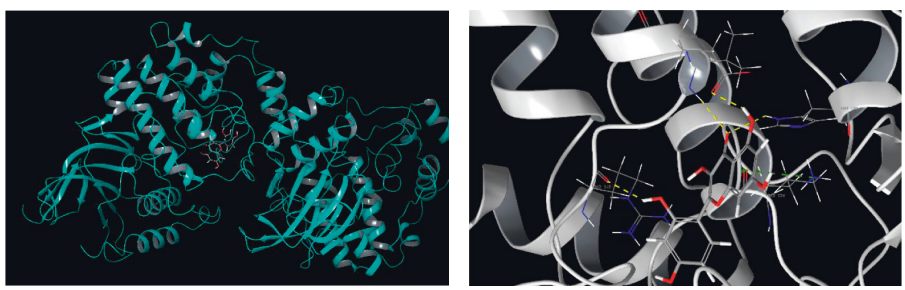

MAPK3-Rosmarinic acid

Figure 3: Molecular docking of active components of FSL with core targets. The yellow dotted line represents H-bond, and the green dotted line represents Pi-cation.

protein kinase 1; AKT1, AKT serine/threonine kinase 1; MAPK3, mitogen-activated protein kinase 3.

3.5. Determination of the $TCID_{50}$ of RSV and the Toxicity of Drugs to HEp-2. The determination of $TCID_{50}$ is as follows: Calculate the $TCID_{50}$ of RSV to be $10^{-5.67}/100\,\mu L$.

Determination of the maximum nontoxic concentration of the active ingredients of Forsythia suspensa leaf is as follows: The toxicity of the five compounds and the positive drug ribavirin to HEp-2 cells showed that most cells were broken or detached, and the cell growth rate was significantly reduced. Cell survival rate >90% was selected as the TC_0 of each administration group on HEp-2 cells, and the TC_0 of each administration group on HEp-2 cells was also measured (Table 3).

3.6. Anti-RSV Efficacy of the Active Ingredients of Forsythia Suspense Leaf. Compared with the normal group, the OD value of the model group was significantly reduced at 24 h and 48 h after RSV infected, and the HEp-2 cells had obvious lesions; compared with the model group, the OD value and the number of cells increased significantly at each concentration of each drug group and ribavirin group at 24 h, but after 48 h, there was no significant difference between each administration group and model group. The 24 h cell survival rate showed that the rate of the model group was (21.62 ± 4.40) %, significantly lower than that of the normal group ($^{*}P < 0.05$). Compared with the model group, the cell survival rates in the phillyrin and rosmarinic acid groups were significantly increased ($^{\#}P < 0.05$), indicating that the effective components of phillyrin and rosmarinic acid in Forsythia suspense leaf could improve the cell survival rate of RSV infection and effectively inhibit the proliferation of RSV(Figure 4). According to the results of the enrichment pathway in 3.3, phillyrin and rosmarinic acid were selected for Western blot verification of PI3K/AKT channel protein.

3.7. Effect of Drugs on PI3K/AKT Signaling Pathway in HEp-2 Cells by Western Blot. Compared with the normal group, the relative expression level of AKT in the model group was significantly increased($^{*}P < 0.05$), and the relative expression levels of PI3K and p-PI3K were significantly decreased ($^{*}P < 0.05$). Compared with the model group, the relative expression level of AKT in the phillyrin group was significantly decreased ($^{\#}P < 0.05$), and the relative expression levels of PI3K and p-PI3K were significantly increased ($^{\#}P < 0.05$). The relative expression level of AKT in the Rosmarinic acid group was significantly decreased ($^{\#}P < 0.05$), and the relative expression level of PI3K was significantly increased ($^{\#}P < 0.05$) (Figure 5).

4. Discussion

RSV is the most common pathogen of viral pneumonia in children, which can cause interstitial pneumonia, bronchiolitis, and other inflammatory diseases, and reinfection is very common, unfortunately, there is still no approved RSV vaccine in China. In recent years, studies on traditional Chinese medicine and its preparations have shown that traditional Chinese medicine has unique advantages in antiviral owing to its many action targets and low incidence of drug resistance. [41] In China, FSL has a long history as tea. It has various chemical components, including phenyl ethanol and its glycosides, lignans and its glycosides, volatile oil, and other chemical substances, [42] among them, a variety of traditional Chinese medicine preparations containing phillyrin have been proved to have significant anti-RSV effects, which reveal that FSL has potential anti-RSV value. In this study, the combination of network pharmacology and experimental verification was used to explore the active components and mechanism of anti-RSV.

Table 3: TC_0 on HEp-2 cells in each administration group ($n = 6$).

Name	TC_0 (μg/mL)
Cryptochlorogenic acid	125
Phillygenin	250
Phillyrin	1000
Rosmarinic acid	250
Rutin	500
Ribavirin	250

TC_0, maximal atoxic concentration.

In this paper, the method of network pharmacology combined with molecular docking was used to explore the complex network of multicomponent, multitarget, and multipathway of anti-RSV processes in FSL. Firstly, 67 compounds were isolated and identified from the decoction of FSL by LC-MS, and then 2952 targets of FSL, 849 targets of RSV pneumonia, and 169 targets of the anti-RSV potential of the active components in FSL were screened. The results of the PPI network analysis showed that FSL may play an anti-RSV effect by regulating target proteins, for example, TP53, STAT3, MAPK1, AKT1, MAPK3, MAPK8, SRC, TNF, and so on. GO enrichment analysis showed that the biological process of RSV resistance of FSL involved protein binding, nucleus, cytosol, cytoplasm, and plasma membrane. KEGG pathway enrichment analysis showed that pathways in cancer, PI3K/AKT signaling pathway, proteoglycans in cancer, and hepatitis B pathways played an important role. The results of docking between the active components of FSL and the main target protein molecules showed that cryptochlorogenic acid, phillyrin, phillyringenin, rutin, and rosmarinic acid had higher binding activities to TP53, STAT3, MAPK1, AKT1, and MAPK3, respectively. *In vitro* antiviral experiments of water extract of FSL and five active components in FSL show that water extract of FSL and active components phillyrin and rosmarinic acid have obvious RSV inhibition effect, and the anti-RSV effect of water extract of FSL is better than that of the two active components. It is speculated that the antiviral effect of FSL is the result of the interaction and synergy of various active components.

According to the results of GO enrichment analysis and KEGG pathway enrichment analysis, the PI3K/AKT signal pathway may have potential value in the anti-RSV treatment of FSL; therefore, PI3K/AKT signal pathway is selected for

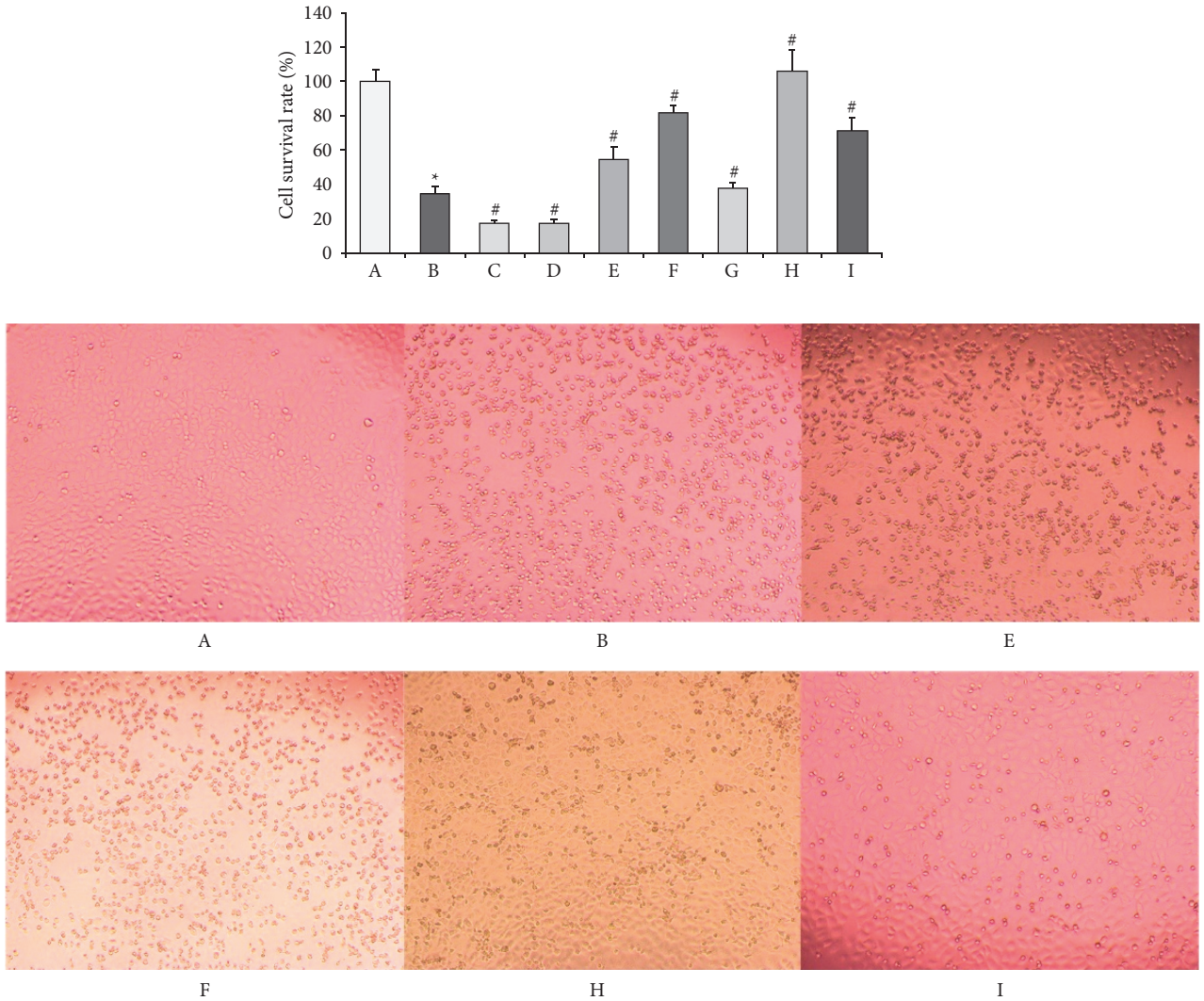

Figure 4: The effect of the active ingredients of FSL on the survival rate of RSV-infected HEp-2 cells($\bar{x} \pm s$, $n = 6$) (a). Normal group; (b) model group; (c) 125 μg/mL cryptochlorogenic acid; (d) 62.5 μg/mL *phillyringenin*; (e) 1000 μg/mL *phillyrin*; (f) 125 μg/mL rosmarinic acid; (g) 62.5 μg/mL rutin; (h) 2500 μg/mL water extract of FSL; (I) 250 μg/mL ribavirin; compared with normal group $^{*}P < 0.05$; compared with model group $^{\#}P < 0.05$.

further study. Western blotting experiments show that the relative expression level of AKT in the phillyrin group was significantly decreased, while the relative expression level of PI3K and p-PI3K was significantly increased. The relative expression level of AKT in the rosmarinic acid group decreased significantly, while the relative expression level of PI3K increased significantly, suggesting that the anti-RSV effect of FSL may be related to the inhibition of the PI3K/AKT pathway. Studies have shown that the PI3K/AKT signal pathway plays an important regulatory role in pulmonary inflammatory diseases. Resveratrol can inhibit the activation of the PI3K/AKT signal pathway induced by RSV, reduce the inflammatory response, and thus play a protective role in lung injury caused by RSV. PI3K/AKT pathway is a vital signal transduction pathway in cells, which can regulate cell differentiation, proliferation, activation, and antiviral ability through the expression of a series of protein factors [43, 44]. PI3K (phosphatidylinositol-3-kinase) is a dimer composed of regulatory subunit p85 and catalytic subunit p110. After activation, a second messenger PIP3 (phosphatidylinositol-3-phosphate) is produced on the plasma membrane. PIP3 can change the protein structure of AKT and activate it, and activate or inhibit the activity of a series of downstream substrates, such as apoptosis-related proteins Bad and caspase 9 by phosphorylation, thereby regulating cell proliferation, differentiation, apoptosis, and migration. [45, 46] Therefore, the activation of the PI3K/AKT signal pathway can reduce the effect of apoptosis and prolong the survival time of cells. On the one hand, RSV infection can up-regulate S1P (sphingosine 1-phosphate) [47], which can mediate the activation of the AKT pathway and up-regulate the expression of the Mdm-2 gene, thus mediating the degradation of tumor suppressor gene p53 and promoting the cell survival time. On the other hand, it can also directly activate PI3K/AKT signaling pathway and inhibit cell apoptosis [48] (Figure 6), thus facilitating the virus to complete its own life

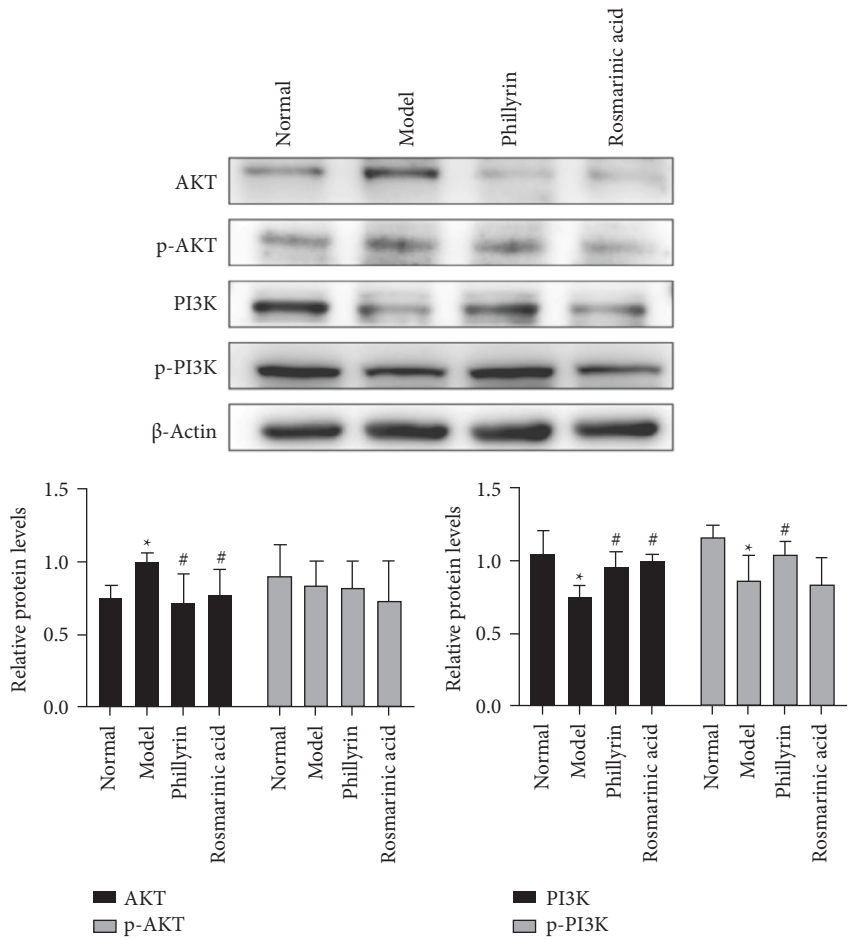

Figure 5: Effects of rosmarinic acid and *phillyrin* on PI3K/AKT signaling pathway-related proteins ($\bar{x} \pm s$, $n = 3$).

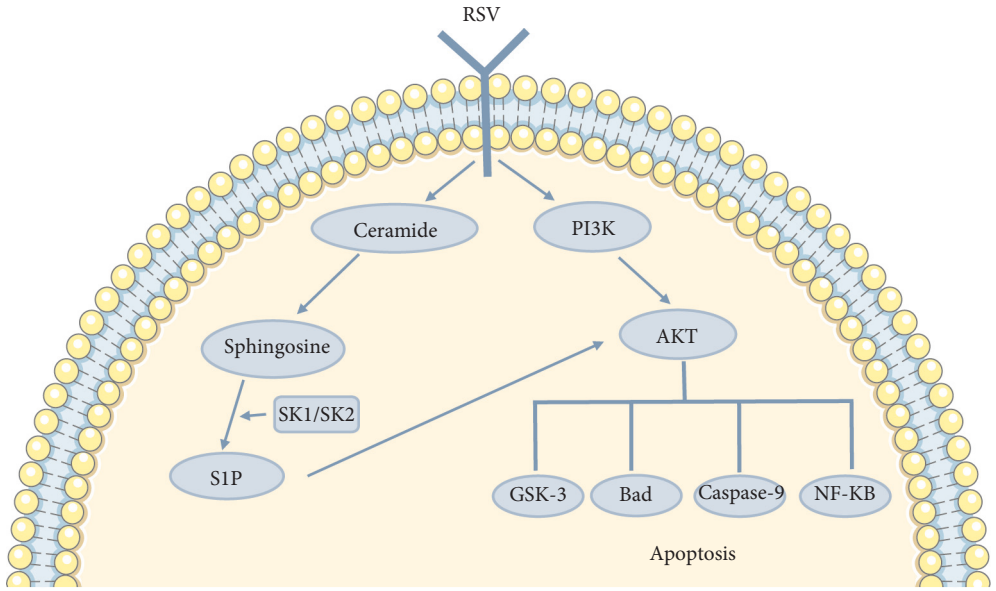

Figure 6: Model for prolonged cell survival after RSV infection.

cycle for amplification before cell apoptosis. [49, 50] It can be speculated that the active components in FSL promote apoptosis and shorten cell survival time by inhibiting PI3K/AKT signal pathway, so as to play an anti-RSV role.

The present study has several limitations. Firstly, due to the continuous updating of the network pharmacology database, there may be a lack of up-to-date bioactive components and target genes in this study. In addition, other

signal pathways may also be involved in the anti-RSV effect of active components in FSL, which needs to be verified by more experiments. Finally, the solubility of phillyrin reduces its efficacy *in vitro*, and more studies are needed to further explore the molecular mechanism of phillyrin against RSV in *vivo*.

5. Conclusion

To sum up, based on network pharmacology combined with the molecular docking method, this study explored the active ingredients and potential mechanism of FSL against RSV through *in vitro* experiments. The results showed that phillyrin and rosmarinic acid in FSL could inhibit PI3K/AKT signaling pathway, promote cell apoptosis and shorten cell survival time, thus playing an anti-RSV role. This study can not only provide a theoretical basis and experimental support for the further development and application of FSL and its effective components in the future but also provide a promising way to reveal the scientific basis and treatment mechanism of diseases treated by traditional Chinese medicine.

Data Availability

All data used to support the findings of this study are included within the article.

Conflicts of Interest

The authors declare no conflicts of interest.

Authors' Contributions

Xiaoxue Wang, Ping Wang, and Haitao Du designed the study. The extraction of FSL was performed by Ru Zhang and Wanying Qi. Na Li, Tianyuan Jing, and Yanan Hu conducted cell experiments. The molecular docking was performed by Tianyu Liu and Lanxin Zhang. Huimin Zhang and Nan Xu analyzed the data. Xiaoxue Wang and Haitao Du drafted the article. Ping Wang, Yi Wang, and Xiaoyan Ding revised the article. All the authors read and approved the final manuscript. Xiaoxue Wang, Ping Wang and Haitao Du authors contributed equally.

Acknowledgments

This research was funded by the National Key R&D Program of China (2019YFE0117800), Central Special Fund for Guiding Local Science and Technology Development (YDZX2021117); Shandong Provincial Key R&D Plan (Science and Technology Demonstration Project) (2021SFGC1205); the Major Science and Technology Innovation Projects of Shandong Province (2020CXGC010505-04 and 2018CXGC1310); the Natural Foundation of Shandong Province (ZR2020MH386 and ZR2019MH134); Collaborative Innovation Center for Quality Control and Whole Industry Chain Construction of Traditional Chinese Medicine in Colleges and Universities of Shandong Province (CYLXTCX2021-01); Central Government Guides Local Projects (YDZX20203700002055), and National Innovation Key Talents Training Project of Traditional Chinese Medicine.

Supplementary Materials

Supplementary Table 1. Main chemical composition of FSL. The optimal binding energy location of the target protein. (*Supplementary Materials*)

References

[1] C. Johansson, "Respiratory syncytial virus infection: an innate perspective," *F1000Research*, vol. 5, p. 2898, 2016.

[2] A. T. Borchers, C. Chang, M. E. Gershwin, and L. J. Gershwin, "Respiratory syncytial virus--a comprehensive review," *Clinical Reviews in Allergy and Immunology*, vol. 45, no. 3, pp. 331–379, 2013.

[3] G. Wang, J. Deval, J. Hong et al., "Discovery of 4′-chloromethyl-2′-deoxy-3′,5′-di-O-isobutyryl-2′-fluorocytidine (ALS-8176), a first-in-class RSV polymerase inhibitor for treatment of human respiratory syncytial virus infection," *Journal of Medicinal Chemistry*, vol. 58, no. 4, pp. 1862–1878, 2015.

[4] N. Friedman, H. Alter, M. Hindiyeh, E. Mendelson, Y. Shemer Avni, and M. Mandelboim, "Human coronavirus infections in Israel: epidemiology, clinical symptoms and summer seasonality of HCoV-HKU1," *Viruses*, vol. 10, p. 515, 2018.

[5] E. Caffrey Osvald and J. R. Clarke, "NICE clinical guideline: bronchiolitis in children," *Archives of Disease in Childhood: Education and Practice*, vol. 101, no. 1, pp. 46–48, 2016.

[6] S. C. Ma, J. Du, P. P. H. But et al., "Antiviral chinese medicinal herbs against respiratory syncytial virus," *Journal of Ethnopharmacology*, vol. 79, no. 2, pp. 205–211, 2002.

[7] H. Shi, K. Ren, B. Lv et al., "Baicalin from scutellaria baicalensis blocks respiratory syncytial virus (RSV) infection and reduces inflammatory cell infiltration and lung injury in mice," *Scientific Reports*, vol. 6, no. 1, Article ID 35851, 2016.

[8] W. Li, L. T. Sun, L. Zhao, X. D. Yue, and S. J. Dai, "New C9-monoterpenoid alkaloids featuring a rare skeleton with anti-inflammatory and anti-viral activities from forsythia suspensa," *Chemistry & Biodiversity*, vol. 19, 2021.

[9] Z. Han, X. L. Lei, H. Zhang et al., "Evaluating the safety of forsythin from forsythia suspensa leaves by acute and subchronic oral administration in rodent models," *Asian Pacific Journal of Tropical Medicine*, vol. 10, no. 1, pp. 47–51, 2017.

[10] Q. Ma, R. Li, W. Pan et al., "Phillyrin (KD-1) exerts anti-viral and anti-inflammatory activities against novel coronavirus (SARS-CoV-2) and human coronavirus 229E (HCoV-229E) by suppressing the nuclear factor kappa B (NF-κB) signaling pathway," *Phytomedicine*, vol. 78, 2020.

[11] W. T. Zhong, Y. C. Wu, X. X. Xie et al., "Phillyrin attenuates LPS-induced pulmonary inflammation via suppression of MAPK and NF-κB activation in acute lung injury mice," *Fitoterapia*, vol. 90, pp. 132–139, 2013.

[12] S. Zhou, A. Zhang, and W. Chu, "Phillyrin is an effective inhibitor of quorum sensing with potential as an anti-Pseudomonas aeruginosa infection therapy," *Journal of Veterinary Medical Science*, vol. 81, no. 3, pp. 473–479, 2019.

[13] X. Y. Qu, Q. J. Li, H. M. Zhang et al., "Protective effects of phillyrin against influenza a virus in vivo," *Archives of Pharmacal Research*, vol. 39, no. 7, pp. 998–1005, 2016.

[14] Y. Ge, Y. Wang, P. Chen et al., "Polyhydroxytriterpenoids and phenolic constituents from Forsythia suspensa (thunb.) vahl

leaves," *Journal of Agricultural and Food Chemistry*, vol. 64, no. 1, pp. 125–131, 2016.

[15] W. Sun, Y. Chen, and M. Li, "Systematic elaboration of the pharmacological targets and potential mechanisms of ZhiKe GanCao decoction for preventing and delaying intervertebral disc degeneration," *Evidence-based Complementary and Alternative Medicine*, vol. 2022, pp. 1–11, 2022.

[16] Y. Ju, "The mechanism of osthole in the treatment of gastric cancer based on network pharmacology and molecular docking technology," *Applied Bionics and Biomechanics*, vol. 2022, pp. 1–8, 2022.

[17] H. Du, J. Ding, P. Wang et al., "Anti-respiratory syncytial virus mechanism of houttuynia cordata thunb exploration based on network pharmacology," *Comb Chem High Throughput Screen*, vol. 24, 2020.

[18] Z. Zhou, B. Chen, S. Chen et al., "Applications of network pharmacology in traditional chinese medicine research," *Evidence-based Complementary and Alternative Medicine*, vol. 2020, pp. 1–7, 2020.

[19] A. Daina, O. Michielin, and V. Zoete, "SwisstargetPrediction: updated data and new features for efficient prediction of protein targets of small molecules," *Nucleic Acids Research*, vol. 47, pp. W357–W364, 2019.

[20] S. J. Huang, F. Mu, F. Li et al., "Systematic elucidation of the potential mechanism of erzhi pill against drug-induced liver injury via network pharmacology approach," *Evidence-based Complementary and Alternative Medicine*, vol. 2020, pp. 1–15, 2020.

[21] X. Huang, M. Zhang, H. Wu, X. Wang, and F. Xu, "The study on the active ingredients and potential targets of rice bran petroleum ether extracts for treating diabetes based on network pharmacology," *Combinatorial Chemistry & High Throughput Screening*, vol. 24, no. 6, pp. 790–802, 2021.

[22] F. Hufsky, K. Lamkiewicz, A. Almeida et al., "Computational strategies to combat COVID-19: useful tools to accelerate SARS-CoV-2 and coronavirus research," *Briefings in Bioinformatics*, vol. 22, no. 2, pp. 642–663, 2021.

[23] S. Pundir, M. J. Martin, and C. O'Donovan, "UniProt protein knowledgebase," *Methods in Molecular Biology*, vol. 1558, pp. 41–55, 2017.

[24] L. Hu, Y. Chen, T. Chen, D. Huang, S. Li, and S. Cui, "A systematic study of mechanism of sargentodoxa cuneata and patrinia scabiosifolia against pelvic inflammatory disease with dampness-heat stasis syndrome via network pharmacology approach," *Frontiers in Pharmacology*, vol. 11, Article ID 582520, 2020.

[25] R. Barshir, S. Fishilevich, T. Iny-Stein et al., "GeneCaRNA: a comprehensive gene-centric database of human non-coding RNAs in the GeneCards suite," *Journal of Molecular Biology*, vol. 433, no. 11, Article ID 166913, 2021.

[26] J. S. Amberger and A. Hamosh, "Searching online mendelian inheritance in man (OMIM): a knowledgebase of human genes and genetic phenotypes," *Current Protocols in Bioinformatics*, vol. 58, pp. 1.2.1–1.2.12, 2017.

[27] Z. Zhang, J. Liu, Y. Liu, D. Shi, Y. He, and P. Zhao, "Virtual screening of the multi-gene regulatory molecular mechanism of Si-Wu-tang against non-triple-negative breast cancer based on network pharmacology combined with experimental validation," *Journal of Ethnopharmacology*, vol. 269, Article ID 113696, 2021.

[28] N. T. Doncheva, J. H. Morris, J. Gorodkin, and L. J. Jensen, "Cytoscape stringapp: network analysis and visualization of proteomics data," *Journal of Proteome Research*, vol. 18, no. 2, pp. 623–632, 2019.

[29] P. Shannon, A. Markiel, O. Ozier et al., "Cytoscape: a software environment for integrated models of biomolecular interaction networks," *Genome Research*, vol. 13, no. 11, pp. 2498–2504, 2003.

[30] A. He, W. Wang, Y. Xia, and X. Niu, "A network pharmacology approach to explore the mechanisms of artemisiae scopariae herba for the treatment of chronic hepatitis B," *Evidence-based Complementary and Alternative Medicine*, vol. 2021, pp. 1–10, 2021.

[31] D. Szklarczyk, A. L. Gable, K. C. Nastou et al., "The String database in 2021: customizable protein-protein networks, and functional characterization of user-uploaded gene/measurement sets," *Nucleic Acids Research*, vol. 49, pp. D605–D612, 2021.

[32] D. W. Huang, B. T. Sherman, Q. Tan et al., "DAVID bioinformatics resources: expanded annotation database and novel algorithms to better extract biology from large gene lists," *Nucleic Acids Research*, vol. 35, pp. W169–W175, 2007.

[33] D. W. Huang, B. T. Sherman, and R. A. Lempicki, "Systematic and integrative analysis of large gene lists using DAVID bioinformatics resources," *Nature Protocols*, vol. 4, no. 1, pp. 44–57, 2009.

[34] M. Liu, G. Fan, D. Zhang, M. Zhu, and H. Zhang, "Study on mechanism of jiawei chaiqin wendan decoction in treatment of vestibular migraine based on network pharmacology and molecular docking technology," *Evidence-based Complementary and Alternative Medicine*, vol. 2021, pp. 1–12, 2021.

[35] Z. Li, Y. Zhang, Y. Zhou et al., "Tanshinone IIA suppresses the progression of lung adenocarcinoma through regulating CCNA2-CDK2 complex and AURKA/PLK1 pathway," *Scientific Reports*, vol. 11, no. 1, Article ID 23681, 2021.

[36] L. Breuza, S. Poux, A. Estreicher et al., "The UniProtKB Guide to the Human Proteome," *Database (Oxford)*, vol. 2016, 2016.

[37] P. Indu, N. Arunagirinathan, M. R. Rameshkumar, K. Sangeetha, A. Divyadarshini, and S. Rajarajan, "Antiviral activity of astragaloside II, astragaloside III and astragaloside IV compounds against dengue virus: computational docking and in vitro studies," *Microbial Pathogenesis*, vol. 152, Article ID 104563, 2021.

[38] J. C. Stockert, A. Blazquez-Castro, M. Canete, R. W. Horobin, and A. Villanueva, "MTT assay for cell viability: intracellular localization of the formazan product is in lipid droplets," *Acta Histochemica*, vol. 114, no. 8, pp. 785–796, 2012.

[39] G. Gallo-Oller, R. Ordonez, and J. Dotor, "A new background subtraction method for western blot densitometry band quantification through image analysis software," *Journal of Immunological Methods*, vol. 457, pp. 1–5, 2018.

[40] H. Tao, J. Zhong, Y. Mo, W. Liu, and H. Wang, "Exploring the mechanism through which Phyllanthus emblica L. Extract exerts protective effects against acute gouty arthritis: a network pharmacology study and experimental validation," *Evidence-based Complementary and Alternative Medicine*, vol. 2022, pp. 1–16, 2022.

[41] Y. Liu, J. Zhao, Y. Guo, M. Wang, X. Li, and B. Zhang, "Mutagenic and teratogenic toxicity evaluation of forsythia suspensa leaves aqueous extract," *Drug and Chemical Toxicology*, vol. 45, no. 4, pp. 1825–1832, 2021.

[42] M. Tokar and B. Klimek, "The content of lignan glycosides in forsythia flowers and leaves," *Acta Poloniae Pharmaceutica*, vol. 61, no. 4, pp. 273–278, 2004.

[43] R. Katso, K. Okkenhaug, K. Ahmadi, S. White, J. Timms, and M. D. Waterfield, "Cellular function of phosphoinositide 3-kinases: implications for development, immunity, homeostasis,

and cancer," *Annual Review of Cell and Developmental Biology*, vol. 17, no. 1, pp. 615–675, 2001.

[44] J. Downward, "Mechanisms and consequences of activation of protein kinase B/akt," *Current Opinion in Cell Biology*, vol. 10, no. 2, pp. 262–267, 1998.

[45] R. Yao and G. M. Cooper, "Requirement for phosphatidylinositol-3 kinase in the prevention of apoptosis by nerve growth factor," *Science*, vol. 267, no. 5206, pp. 2003–2006, 1995.

[46] G. Song, G. Ouyang, and S. Bao, "The activation of akt/PKB signaling pathway and cell survival," *Journal of Cellular and Molecular Medicine*, vol. 9, no. 1, pp. 59–71, 2005.

[47] M. M. Monick, K. Cameron, L. S. Powers et al., "Sphingosine kinase mediates activation of extracellular signal-related kinase and akt by respiratory syncytial virus," *American Journal of Respiratory Cell and Molecular Biology*, vol. 30, no. 6, pp. 844–852, 2004.

[48] K. W. Thomas, M. M. Monick, J. M. Staber, T. Yarovinsky, A. B. Carter, and G. W. Hunninghake, "Respiratory syncytial virus inhibits apoptosis and induces NF-kappa B activity through a phosphatidylinositol 3-kinase-dependent pathway," *Journal of Biological Chemistry*, vol. 277, no. 1, pp. 492–501, 2002.

[49] V. Bitko, O. Shulyayeva, B. Mazumder et al., "Nonstructural proteins of respiratory syncytial virus suppress premature apoptosis by an NF-κB-Dependent, interferon-independent mechanism and facilitate virus growth," *Journal of Virology*, vol. 81, no. 4, pp. 1786–1795, 2007.

[50] D. J. Groskreutz, M. M. Monick, T. O. Yarovinsky et al., "Respiratory syncytial virus decreases P53 protein to prolong survival of airway epithelial cells," *The Journal of Immunology*, vol. 179, no. 5, pp. 2741–2747, 2007.